

Ultra-short period planets: opportunities and challenges for phase-curve spectroscopy

Giuseppe Morello (1,2), Camilla Danielski (1), Pascal Tremblin (1), Marine Martin-Lagarde (1), Daniel Dicken (1), and Pierre-Olivier Lagage (1)
(1) AIM, CEA-Saclay, France, (2) INAF, Italy (giuseppe.morello@cea.fr)

Abstract

We discuss the full phase-curve observations of three hot Jupiters obtained with *HST*/WFC3 at 1.1–1.7 μm and with *Spitzer*/IRAC at 3.6 and 4.5 μm . A careful correction of the instrumental systematics is paramount to obtain robust scientific results, whereas some datasets were debated in the previous literature. We propose several tests, in addition to the most common practices of residuals analysis, to assess the robustness of the results. Another challenge is to finding the atmospheric model that best explains the observations at all wavelengths simultaneously. As a preliminary approach, we (1) generated a grid of atmospheric models for each planet, (2) investigated the relationships between the model-atmospheric parameters and the observable phase-curve properties, and (3) constrained the range of acceptable parameters to match the observations. Finally, we briefly discuss the lessons learned and the desirable steps forward in view of the upcoming *JWST* and *ARIEL* missions.

1. Introduction

Exoplanet phase-curves are measurements of the flux coming from a star+exoplanet system as a function of the orbital phase. The exoplanetary flux includes stellar reflected light and thermal emission with varying phase angle. Exoplanets with short orbital periods are expected to be tidally-locked to their host star, therefore exhibiting a hotter day-side and a cooler nightside. The day-night temperature contrast depends on the heat recirculation efficiency of the exoplanetary atmosphere. Numerical simulations also predict a hotspot offset from the substellar point [Showman & Guillot 2002, Schwartz et al. 2017, Zhang & Showman 2017]. If the system is nearly edge-on, its phase-curve may contain both exoplanetary transit and eclipse events.

Multiwavelength observations of the exoplanetary transits and eclipses are now routinely used to probe

their chemistry, vertical thermal profile and clouds coverage (e.g., [Sing et al. 2016, Tsiaras et al. 2018]). In addition, the phase-curve modulations can be used to further constrain the horizontal distribution and dynamics of the exoplanetary atmospheres. The greater information content comes at the cost of time to monitor the flux over the entire orbit. Ultra-short period planets, i.e., planets with orbital periods below one day, are the most favorable targets for spectroscopic studies of their phase-curve modulations.

2. The case of WASP43 b

WASP43 b is a hot Jupiter orbiting around a K7 V star in \sim 19.5 hours [Hellier et al. 2011]. Three full phase-curves of WASP43 b have been observed with *HST*/WFC3 at 1.1–1.7 μm [Stevenson et al. 2014], two phase-curves with *Spitzer*/IRAC at 3.6 μm and one phase-curve at 4.5 μm [Stevenson et al. 2017]. Another full phase-curve observation of WASP43 b is planned as part of the Transiting Exoplanet Community ERS program of the *JWST* using MIRI [Bean et al. 2018].

[Stevenson et al. 2014] and [Stevenson et al. 2017] claimed extremely low circulation efficiency for the atmosphere of WASP43 b: $\varepsilon = 0.002^{+0.01}_{-0.002}$, where ε is the night-day bolometric flux ratio. However, they discarded the first 3.6 μm dataset, which presented discrepant results, and larger correlated noise in the light-curve residuals. We [Morello et al. 2019] reanalysed the three *Spitzer*/IRAC phase-curves, finding higher nightside temperatures, smaller hotspot offsets, and greater consistency ($\sim 1\sigma$) between the two 3.6 μm visits than those reported by [Stevenson et al. 2017]. Our results point towards a greater circulation efficiency of the WASP43 b atmosphere, in agreement with an empirical trend between irradiation temperature and circulation efficiency. Additionally, we compared the observed phase-curves with a grid of atmospheric models, finding a good agreement ($\sim 2\sigma$) with a range of models with metallicity between 1 \times

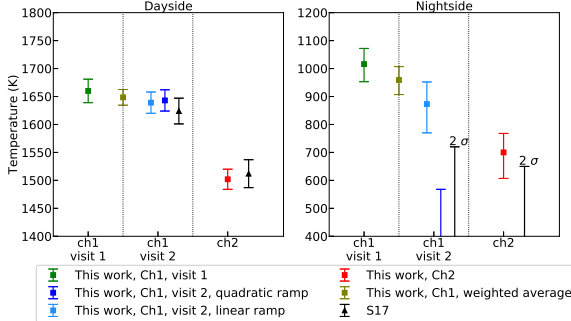


Figure 1: Left: Maximum dayside temperatures obtained in this work for the first $3.6\text{ }\mu\text{m}$ visit (green), second $3.6\text{ }\mu\text{m}$ visit using a quadratic (blue) or linear (dodgerblue) ramp model, weighted average between the first and second visit with a linear ramp (olive), $4.5\text{ }\mu\text{m}$ visit (red), and temperatures reported by [Stevenson et al. 2017] (black triangles). Right: Analogous plot for the minimum nightside temperatures. [Stevenson et al. 2017] only reported 2σ upper limits for the nightside temperatures.

and $3\times$ solar, and cloud top pressure of $\sim 10^{-2}$. Our phase-curve parameter results are consistent within 1σ with those reported in a recent reanalysis by [Mendonça et al. 2018], but we provide an alternative interpretation with a lower cloud top pressure instead of invoking a strong disequilibrium chemistry. [Mendonça et al. 2018b] could not physically explain that chemical disequilibrium.

3. Summary and Conclusions

Phase-curve spectroscopy enables characterisation of the exoplanet atmospheres with a much greater detail than transit/eclipse spectroscopy, potentially breaking many model degeneracies. Three ultra-short period Jupiters are the only planets for which a spectrally-resolved light-curve has been observed to date. We discussed the scientific results obtained and the main challenges encountered in the analyses. These preliminary studies are useful to optimise the scientific return of the upcoming JWST and ARIEL missions.

References

[Bean et al. 2018] Bean, J. L., Stevenson, K. B., Batalha, N. M., et al., 2018, PASP, 130, 114402.

[Hellier et al. 2011] Hellier, C., Anderson, D. R., Collier Cameron, A., et al., 2011, A&A, 535, L7.

[Mendonça et al. 2018] Mendonça, J. M., Malik, M., Demory, B.-O., and Heng, K., 2018, AJ, 155, 150.

[Mendonça et al. 2018b] Mendonça, J. M., Tsai, S.-M., Malik, M., Grimm, S. L., and Heng, K., 2018, AJ, 869, 107.

[Morello et al. 2019] Morello, G., Danielski, C., Dickens, D., Tremblin, P., and Lagage, P.-O., 2019, AJ, 157, 205.

[Schwartz et al. 2017] Schwartz, J. C., Kashner, Z., Jovmir, D., and Cowan, N. B., 2017, ApJ, 850, 154.

[Showman & Guillot 2002] Showman, A. P., and Guillot, T., 2002, A&A, 385, 166.

[Sing et al. 2016] Sing, D. K., Fortney, J. J., Nikolov, N., et al., 2016, Nature, 529, 59.

[Stevenson et al. 2014] Stevenson, K. B., D'sert, J.-M., Line, M. R., et al., 2014, Science, 346, 838.

[Stevenson et al. 2017] Stevenson, K. B., Line, M. R., Bean, J. L., et al., 2014, AJ, 153, 68.

[Tsiaras et al. 2018] Tsiaras, A., Waldmann, I. P., Zingales, T., et al., 2018, AJ, 155, 156.

[Zhang & Showman 2017] Zhang, X., and Showman, A. P., 2017, ApJ, 836, 73.

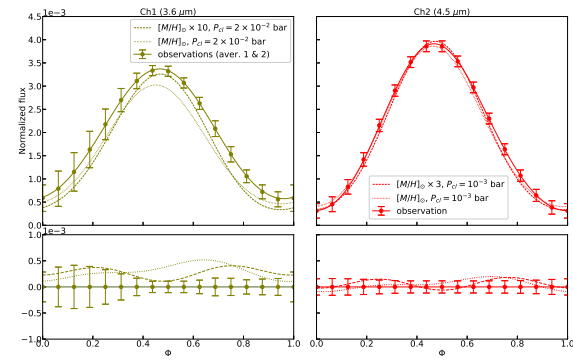


Figure 2: Left, top panel: Observed $3.6\text{ }\mu\text{m}$ phase-curve profile (continuous line and points with error bars), i.e., average of the best-fit profiles for the two visits, the best match from our grid of atmospheric phase-curve models (dashed line), and the best match with solar metallicity (dotted line). The larger error bars for $\Phi < 0.5$ take into account the discrepancy between the best-fit profiles for the two visits. Left, bottom panel: Residuals between the observed and two model phase-curves. Right panels: Analogous plots for the $4.5\text{ }\mu\text{m}$ phase-curve.